# CoCo-MILP: Inter-Variable Contrastive and Intra-Constraint Competitive MILP Solution Prediction

Tianle Pu $^{1,2*}$ , Jianing Li $^{1,2*}$ , Yingying Gao $^{1*}$ , Shixuan Liu $^{3,1,2}$ , Zijie Geng $^4$ , Haoyang Liu $^4$ , Chao Chen $^{1,2}$ , Changjun Fan $^{1,2\dagger}$ 

<sup>1</sup>College of Systems Engineering, National University of Defense Technology

<sup>2</sup>Laboratory for Big Data and Decision, National University of Defense Technology

<sup>3</sup>College of Computer Science and Technology, National University of Defense Technology

<sup>4</sup>MoE Key Laboratory of Brain-inspired Intelligent Perception and Cognition, University of Science and Technology of China {putl22, lijianing24, gaoyingying21, liushixuan, chenc1997, fanchangjun}@nudt.edu.cn, {zijiegeng, dgyoung}@mail.ustc.edu.cn

#### Abstract

Mixed-Integer Linear Programming (MILP) is a cornerstone of combinatorial optimization, yet solving large-scale instances remains a significant computational challenge. Recently, Graph Neural Networks (GNNs) have shown promise in accelerating MILP solvers by predicting high-quality solutions. However, we identify that existing methods misalign with the intrinsic structure of MILP problems at two levels. At the leaning objective level, the Binary Cross-Entropy (BCE) loss treats variables independently, neglecting their relative priority and yielding plausible logits. At the model architecture level, standard GNN message passing inherently smooths the representations across variables, missing the natural competitive relationships within constraints. To address these challenges, we propose CoCo-MILP, which explicitly models inter-variable Contrast and intra-constraint Competition for advanced MILP solution prediction. At the objective level, CoCo-MILP introduces the Inter-Variable Contrastive Loss (VCL), which explicitly maximizes the embedding margin between variables assigned one versus zero. At the architectural level, we design an Intra-Constraint Competitive GNN layer that, instead of homogenizing features, learns to differentiate representations of competing variables within a constraint, capturing their exclusionary nature. Experimental results on standard benchmarks demonstrate that CoCo-MILP significantly outperforms existing learning-based approaches, reducing the solution gap by up to 68.12% compared to traditional solvers. Our code is available at https://github.com/happypu326/CoCo-MILP.

#### 1 Introduction

Mixed-Integer Linear Programming (MILP) is a cornerstone of combinatorial optimization, with diverse applications in the world (Fan et al. 2020, 2023; Liu et al. 2024b; Pu et al. 2024a,b; Liu et al. 2025c; Wang et al. 2025, 2024). Despite its expressive power, solving MILP instances is fundamentally challenging due to their NP-hard nature. To tackle

Copyright © 2026, Association for the Advancement of Artificial Intelligence (www.aaai.org). All rights reserved.

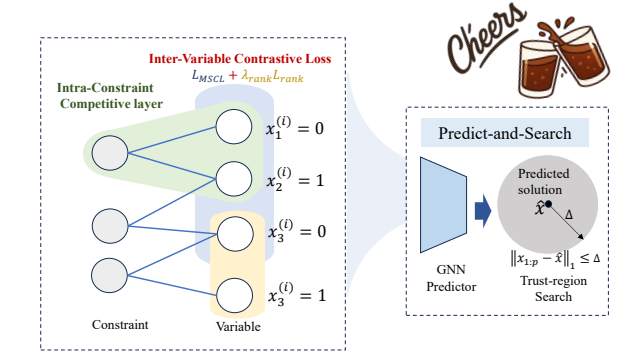


Figure 1: Illustration of CoCo-MILP. We aim to improve the quality of the predicted variables for MILP. The main contribution of our work is the proposed inter-variable contrastive loss and intra-constraint competitive layer for the GNN predictor in the predict-and-search framework.

this, extensive research has led to the development of sophisticated solvers like SCIP (Achterberg 2009) and Gurobi (Gurobi Optimization 2021), which are primarily based on Branch-and-Bound (B&B) and Branch-and-Cut (B&C) algorithms (Land and Doig 2010; Mitchell 2002). Although these solvers are meticulously enhanced with various heuristics, the significant computational burden for large-scale instances remains, motivating the search for new paradigms to accelerate the discovery of high-quality solutions.

A promising paradigm has recently emerged to directly predict high-quality primal solutions using machine learning, particularly Graph Neural Networks (GNNs) (Gasse et al. 2019; Wang et al. 2023). These methods typically frame the task in a supervised learning context: by representing MILP instances as graphs, a GNN is trained to map problem structures to variable assignments, using near-optimal solutions generated by traditional solvers as training labels (Han et al. 2023; Huang et al. 2024; Liu et al. 2025b). This data-driven approach allows the model to learn and exploit structural patterns from past instances to make rapid predic-

<sup>\*</sup>These authors contributed equally.

<sup>&</sup>lt;sup>†</sup>Corresponding author.

tions. Pioneering works, such as Neural Diving (Nair et al. 2020a) and the broader predict-and-search strategies (Han et al. 2023), have shown that leveraging these predictions can significantly accelerate the solving process.

However, despite this considerable potential, the efficacy of these learning-based heuristics is fundamentally limited by their underlying design choices. We identify that the standard GNN architectures and learning objectives are not fully aligned with the combinatorial nature of MILP, which manifests as two critical misalignments. First, at the learning objective level, the prevalent use of the Binary Cross-Entropy (BCE) loss function frames the task as a set of independent binary classifications, one for each variable. This formulation inherently neglects the relative priority among variables, which is critical for constructing a globally optimal solution, and consequently yields plausible but poorly separated logits. Second, at the model architecture level, standard GNN message-passing mechanisms inherently smooth representations, making connected nodes more similar. In the context of MILP, however, variables sharing a constraint (e.g., in  $\sum_{i} x_i \le 1$ ) are often mutually competitive (Chen et al. 2022, 2024a,b; Zhang et al. 2024). The smoothing nature of standard GNNs thus works directly against the goal of capturing these crucial competitive relationships, effectively masking the problem's underlying structure.

To address these challenges, we propose CoCo-MILP, a novel framework designed to explicitly model inter-variable Contrast and intra-constraint Competition. To rectify the objective-level misalignment, CoCo-MILP introduces an Inter-Variable Contrastive Loss (VCL), which moves beyond pointwise accuracy to directly optimize the relative ordering of variables by maximizing the embedding margin between variables assigned one versus zero. In parallel, to address the architectural misalignment, we design an Intra-Constraint Competitive GNN layer. This layer is engineered to differentiate, rather than homogenize, the representations of competing variables within a constraint, enabling the model to effectively learn their exclusionary nature.

#### 2 Preliminaries

## 2.1 Mixed-Integer Linear Programming

A standard Mixed-Integer Linear Programming (MILP) instance  $\mathcal I$  is defined as:

$$\min_{\boldsymbol{x} \in \mathbb{Z}^p \times \mathbb{R}^{n-p}} \left\{ \boldsymbol{c}^{\top} \boldsymbol{x} \mid \boldsymbol{A} \boldsymbol{x} \leq \mathbf{b}, \ \boldsymbol{l} \leq \boldsymbol{x} \leq \boldsymbol{u} \right\}, \tag{1}$$

where  $x \in \mathbb{R}^n$  denotes the decision variables, with the first p entries being integer and the remaining n-p continuous. The vector  $c \in \mathbb{R}^n$  denotes the coefficients of the linear objective, the constraints are defined by the matrix  $A \in \mathbb{R}^{m \times n}$  and the right-hand side vector  $b \in \mathbb{R}^m$ , and the variable bounds are given by  $b \in \mathbb{R}^m$ , and  $b \in \mathbb{R}^m$  and  $b \in \mathbb{R}^m$ . Without loss of generality, we focus on binary integer variables, i.e., we assume that  $b \in \{0,1\}^p \times \mathbb{R}^{n-p}$ . General integer variables can be handled via standard preprocessing techniques (Nair et al. 2020b). Finding the optimal solution that optimizes the objective func-

tion is NP-hard, making large-scale instances computationally challenging for exact solvers.

#### 2.2 Related Work

In recent years, machine learning techniques have seen widespread use in accelerating the solution of MILPs (Li et al. 2024). These research efforts primarily follow four key directions. One focus is on generating new data to support solver advancement (Geng et al. 2023; Liu et al. 2024a). Another critical direction involves enhancing key modules within solvers including variable selection (Gasse et al. 2019; Qu et al. 2022; Kuang et al. 2024), node selection (He, Daume III, and Eisner 2014; Labassi, Chetelat, and Lodi 2022; Zhang et al. 2025), cutting plane selection (Wang et al. 2023; Li et al. 2023; Ye et al. 2025), and large neighborhood search (Sonnerat et al. 2021; Huang et al. 2023; Song et al. 2020; Wu et al. 2021; Ye et al. 2023) A third area of exploration centers on predicting high-quality solutions to enable warm-starting of solvers, as demonstrated in studies such as (Nair et al. 2020b; Han et al. 2023; Huang et al. 2024; Geng et al. 2025; Liu et al. 2025b). Additionally, efforts have been directed at improving the generalization ability of learning-based models (Liu et al. 2023; Ye et al. 2023; Ye, Xu, and Wang 2024; Pu et al. 2025). We also observe that as Large Language Models (LLMs) grow in popularity, a range of LLM-based methods have appeared, and one notable application among these is LLM-driven optimization modeling (Jiang et al. 2024; Liu et al. 2025a). Finally, we provide details on related works in ML4CO and contrastive learning, which are included in Appendix B.

## 2.3 Predict-and-Search Framework for MILPs

We can encode each MILP instance as a bipartite graph  $\mathcal{G}=(\mathcal{W}\cup\mathcal{V},\mathcal{E})$ , where  $\mathcal{W}$  and  $\mathcal{V}$  denote the sets of constraint and variable nodes, respectively, and the edge set  $\mathcal{E}$  corresponds to non-zero entries in A. Each node and edge is associated with a set of features derived from problem coefficients and structural attributes. Such a bipartite graph can completely describe a MILP instance, enabling GNNs to process the instances and predict their solutions.

We adopt the PS paradigm to approximate the solution distribution of a given MILP. Specifically, the distribution is defined via an energy function that assigns lower energy to high-quality feasible solutions and infinite energy to infeasible ones:

$$p(\boldsymbol{x} \mid \mathcal{I}) = \frac{\exp(-E(\boldsymbol{x} \mid \mathcal{I}))}{\sum_{\boldsymbol{x'}} \exp(-E(\boldsymbol{x'} \mid \mathcal{I}))},$$
where  $E(\boldsymbol{x} \mid \mathcal{I}) = \begin{cases} \boldsymbol{c}^{\top} \boldsymbol{x}, & \text{if } \boldsymbol{x} \text{ is feasible,} \\ +\infty, & \text{otherwise.} \end{cases}$  (2)

Our goal is to learning distribution  $p_{\theta}(\boldsymbol{x}|\mathcal{I})$  for a given instance  $\mathcal{I}$ . To make learning tractable, we assume a fully factorized solution distribution over the binary variables, i.e.,  $p_{\theta}(\boldsymbol{x}|\mathcal{I}) = \prod_{i=1}^p p_{\theta}(x_i|\mathcal{I})$ , where  $p_{\theta}(x_i|\mathcal{I})$  denotes the predicted marginal probability for variable  $x_i$ . To do so, we use a GNN model to output a p-dimension vector  $\hat{\boldsymbol{x}} = \boldsymbol{f}_{\theta}(\mathcal{I}) = (\hat{x}_1, \cdots, \hat{x}_p)^{\top} \in [0, 1]^p$ , where  $\hat{x}_j = p_{\theta}(x_j = 1|\mathcal{I})$ . To train the model, we use a weighted set

of feasible solutions  $\{\boldsymbol{x}^{(i)}\}_{i=1}^N$  as supervised signals, where each solution is assigned a weight  $w_i \propto \exp(-\boldsymbol{c}^{\top}\boldsymbol{x}^{(i)})$ . Let  $x_j^{(i)} = p_{\boldsymbol{\theta}}(x_j^{(i)} = 1|\mathcal{I})$ . Then, the training loss function is a binary cross-entropy loss defined as:

$$\mathcal{L}_{BCE}(\boldsymbol{\theta}|\mathcal{I}) = \sum_{i=1}^{N} w_i \cdot \mathcal{L}_{BCE}(\boldsymbol{\theta}|\mathcal{I}, \boldsymbol{x}^{(i)})$$

$$= \sum_{i=1}^{N} w_i \cdot \sum_{j=1}^{p} -\left[x_j^{(i)} \log \hat{x}_j + (1 - x_j^{(i)}) \log(1 - \hat{x}_j)\right].$$
(3)

At inference time, the GNN model outputs a predicted marginal  $\hat{x} \in [0,1]^p$ . A standard MILP solver (e.g., Gurobi or SCIP) is then used to search for a feasible solution in a local neighborhood around  $\hat{x}$  by solving the following trust region problem:

$$\min_{\boldsymbol{x} \in \mathbb{Z}^p \times \mathbb{R}^{n-p}} \left\{ \boldsymbol{c}^{\top} \boldsymbol{x} \mid \boldsymbol{A} \boldsymbol{x} \leq \mathbf{b}, \ \boldsymbol{l} \leq \boldsymbol{x} \leq \boldsymbol{u}, \boldsymbol{x}_{1:p} \in \mathcal{B}(\hat{\boldsymbol{x}}, \Delta) \right\},$$
(4)

where the trust region  $\mathcal{B}(\hat{x}, \Delta) := \{x \in \mathbb{R}^n : ||x_{1:p} - \hat{x}||_1 \le \Delta\}$  constrains the solver to remain close to the predicted binary configuration.

## 3 Motivation

In this section, we motivate our approach by highlighting two fundamental limitations of conventional methods for predicting MILP solutions: (1) their tendency to produce ambiguous logit scores for variables, and (2) their failure to capture the competitive dynamics within constraints. We also provide an extensive motivation analysis from both operations research and application perspectives in Appendix A.

# 3.1 Inter-Variable Logits Ambiguity

A primary goal of a prediction model is to provide a clear signal to a solver about which variables to prioritize. However, we observe that standard models often fail to do so.

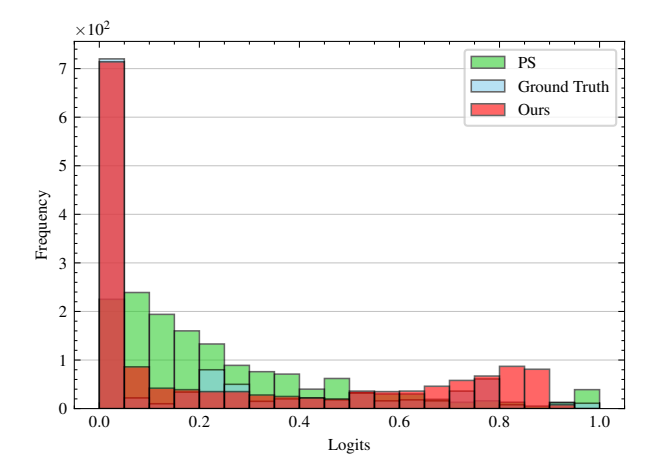


Figure 2: Distribution of Logits from different methods.

**Logits Distribution Visualization.** We begin by visualizing the logit distributions from a baseline GNN model trained with the standard Binary Cross-Entropy (BCE) loss. As shown in Figure 2, the logits produced by PS are poorly separated. The model assigns similar scores to many variables that should be distinguished, failing to establish a clear decision boundary for reliable variable ranking. In contrast, the logits produced by our method exhibit a much clearer separation, aligning better with the ground truth.

Quantifying Logit Separability. To quantify this ambiguity, we measure the model's ability to rank variables correctly. For a given instance, we sample a large number of positive-negative variable pairs  $(v_i, v_j)$  from a ground truth solution, where  $x_i = 1$  and  $x_j = 0$ . We then compute the difference between the predicted scores,  $\Delta_{ij} = \hat{x}_i - \hat{x}_j$ , where  $\hat{x}_i$  and  $\hat{x}_j$  are the predictions for variables  $v_i$  and  $v_j$ , respectively. A positive difference signifies a correct relative ranking, while a negative one indicates an error. The statistics of these differences in Figure 3 reveal that for the baseline model, a substantial portion of the distribution falls into the negative region. This quantitatively confirms that the model is frequently uncertain or even incorrect about the relative importance of variable pairs, underscoring the need for better logit differentiation.

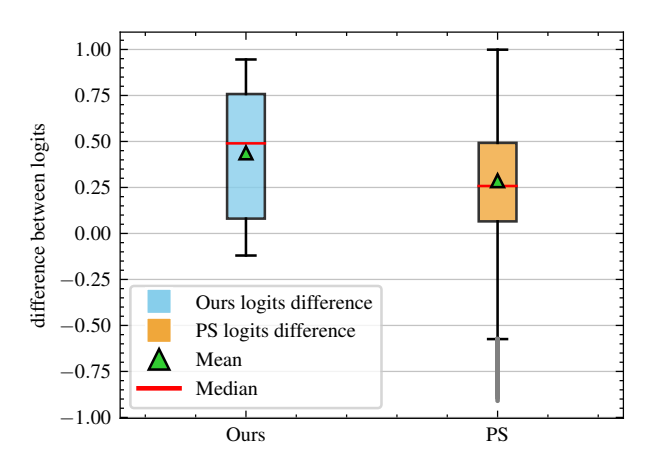


Figure 3: Distribution of the difference between logits corresponding to ground truth 1 and 0 from different methods.

**Analysis.** The standard training objective for MILP solution prediction is the Binary Cross-Entropy (BCE) loss. This objective encourages the model to independently match the marginal probability for each variable. However, a high-quality solution for a MILP problem depends not on individual accuracies, but on the correct *relative ordering* of variables. A solver does not need to know the absolute probability of  $x_i = 1$ ; it needs to know whether  $x_i$  is a *better* candidate than  $x_j$ . A model trained with BCE can be "correct on average" yet fail to create a decisive separation between high- and low-priority variables. This results in ambiguous logits that offer a weak and indecisive signal to the solver, motivating our design of a new loss function that explicitly prioritizes comparative ranking.

# 3.2 Neglect of Intra-Constraint Competitions

A second critical limitation of existing methods is their neglect of the competitive relationships inherent in constraints.

Prevalence of Competition in Constraints. Many constraints, such as the set-packing constraint  $\sum_{i \in S} x_i \leq 1$ , enforce mutual exclusivity, where only one or a few variables can be simultaneously active (i.e., set to 1). To demonstrate the prevalence of this structure, we analyze the activation ratio of constraints across standard benchmark datasets, defined as the proportion of active variables within a constraint in a ground-truth solution. Figure 4 plots the distribution of these activation ratios. The plot reveals that for the vast majority of constraints, the activation ratio is extremely low. This confirms that a "winner-takes-few" or even "winner-takes-one" dynamic is a fundamental and widespread property of MILP instances.

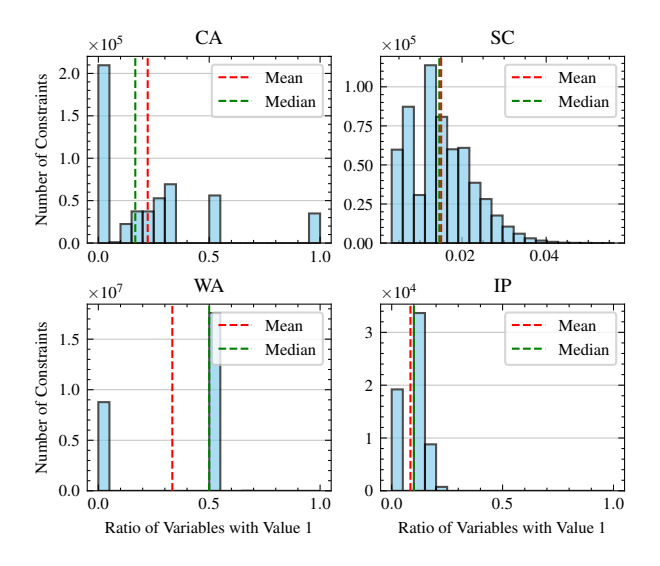


Figure 4: Ratio of variables with value 1 from different problems. For each problem category, we traverse through all constraints to count the number of variables taking the value 1 in the ground truth and plot the resulting histogram.

Insufficient Differentiation within Constraints. We next investigate whether baseline models can capture this competitive structure. An effective model should differentiate between variables within a constraint, assigning high scores to the few "winners" and low scores to the many "losers." We measure this differentiation by calculating the variance of logits among all variables sharing a constraint. Figure 5 compares the distribution of this intra-constraint logit variance for the baseline model against our method. The baseline model's variance is predominantly low, indicating that it assigns indiscriminately similar scores to competing variables. In contrast, our method produces significantly higher variance, demonstrating a superior ability to distinguish between winners and losers within a constraint.

**Analysis.** This failure stems from the core mechanism of the GNNs commonly used for prediction. Standard GNN

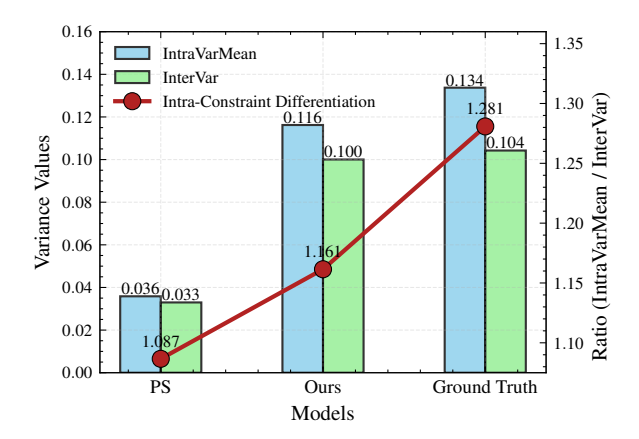


Figure 5: Distribution of logit variance per constraint. IntraVarMean first calculates the variance of logits within each constraint and then computes their average; InterVar calculates the variance across all logits; Ratio represents the ratio of IntraVarMean to InterVar.

message passing is designed to smooth and aggregate features among neighboring nodes. While effective for tasks like node classification, this mechanism is fundamentally ill-suited for modeling competition. By averaging information from neighbors within a constraint, GNNs tend to homogenize the representations of competing variables. This process inherently masks their exclusionary relationships, effectively treating them as collaborators rather than the competitors they are.

# 4 Methodology

Motivated by the observations in Section 3, we propose **CoCo-MILP**, a novel framework that explicitly models inter-variable **Co**ntrast and intra-constraint **Co**mpetition for advanced MILP solution prediction.

#### 4.1 Framework Overview

The CoCo-MILP framework is built upon the PS framework, as introduced in Section 2.3. In the framework, a MILP instance is represented by a variable-constraint bipartite graph, and a GNN is trained to predict the values of binary variables. Our analysis in Section 3 revealed two critical weaknesses in the standard PS approach: the ambiguous variable logits and honogenized representations. We attribute these issues to the inadequate learning objective and the GNN architecture neglecting variable competitions.

CoCo-MILP addresses the aforementioned issues with two core innovations. In Section 4.2, we introduce the Inter-Variable Contrastive Loss (VCL), which replaces the standard BCE loss to learn more discriminative variable logits by focusing on their relative contrast. Then, in Section 4.3, we introduce the Intra-Constraint Competitive (ICC) GNN layer. This layer explicitly models the competitive relationships among variables within shared constraints, thereby counteracting the feature-smoothing effect of standard message passing.

## 4.2 Inter-Variable Contrastive Loss (VCL)

The conventional Binary Cross-Entropy (BCE) loss function treats the prediction for each variable as an independent classification task. This approach disregards the crucial relational context between variables, leading to the ambiguous logits demonstrated in Section 3. To address this, we propose the Inter-Variable Contrastive Loss (VCL), which fundamentally shifts the learning objective from pointwise accuracy to learning discriminative logits. The goal of VCL is to structure the embedding space such that the logits of variables with a ground-truth value of one are systematically and confidently larger than those with a ground-truth value of zero.

Our VCL is a composite objective composed of two complementary loss functions: a global multi-sample contrastive loss and a pairwise ranking loss. For a given MILP instance  $\mathcal{I}$ , let our model with parameters  $\boldsymbol{\theta}$  produce a vector of logits  $\boldsymbol{z}$  and the corresponding prediction  $\hat{\boldsymbol{x}}$ . For a ground-truth solution  $\boldsymbol{x}^{(i)}$ , we partition the set of binary variables  $\mathcal{V}_0$  into a positive set  $\mathcal{V}_+ = \{v_i \mid x_i^{(i)} = 1\}$  and a negative set  $\mathcal{V}_- = \{v_j \mid x_j^{(i)} = 0\}$ . First, we introduce the Multi-Sample Contrastive Loss

First, we introduce the Multi-Sample Contrastive Loss (MSCL), which is inspired by InfoNCE, which adopts a global perspective. It encourages the logits of all positive samples to be collectively larger than the logits of all other variables in the instance. This is formulated as:

$$\mathcal{L}_{\text{MSCL}}(\boldsymbol{\theta} \mid \mathcal{I}, \mathbf{x}^{(i)}) = -\log \frac{\sum_{v_i \in \mathcal{V}_+} \exp(z_i/\tau)}{\sum_{v_k \in \mathcal{V}_0} \exp(z_k/\tau)}, \quad (5)$$

where  $\tau$  is a temperature hyperparameter. This loss pushes the entire group of positive variables away from the entire pool of variables, promoting a coarse-grained separation.

Second, to enforce a more fine-grained separation, we employ a Pairwise Ranking Loss. This loss focuses on the local relationship between every individual positive-negative pair, ensuring a strict margin between their logits. It is defined as:

$$\mathcal{L}_{\text{rank}}(\boldsymbol{\theta} \mid \mathcal{I}, \mathbf{x}^{(i)}) = \frac{1}{|\mathcal{V}_{+}||\mathcal{V}_{-}|} \sum_{v_{i} \in \mathcal{V}_{+}, v_{i} \in \mathcal{V}_{-}} \max(0, \gamma - (z_{i} - z_{j})),$$
 (6)

where  $\gamma > 0$  is a predefined margin. This loss penalizes any pair  $(v_i, v_j)$  where the logit of the positive variable  $z_i$  does not exceed the logit of the negative variable  $z_j$  by at least  $\gamma$ .

The final Inter-Variable Contrastive Loss (VCL) is the weighted sum of these two components:

$$\mathcal{L}_{\text{VCL}}(\boldsymbol{\theta} \mid \mathcal{I}) = \sum_{i=1}^{N} w_i \cdot \mathcal{L}_{\text{VCL}}(\boldsymbol{\theta} \mid \mathcal{I}, \mathbf{x}^{(i)})$$

$$= \sum_{i=1}^{N} w_i \cdot \left[ \mathcal{L}_{\text{MSCL}}(\boldsymbol{\theta} \mid \mathcal{I}, \mathbf{x}^{(i)}) + \lambda_{\text{rank}} \cdot \mathcal{L}_{\text{rank}}(\boldsymbol{\theta} \mid \mathcal{I}, \mathbf{x}^{(i)}) \right],$$
(7)

where  $w_i$  are weights for each solution and  $\lambda_{\text{rank}}$  is a coefficient balancing the two objectives. Unlike BCE, which evaluates each variable in isolation, VCL is relational; its gradient for any single variable depends on the logits of all

other variables. By combining a global contrastive push with fine-grained pairwise ranking, VCL produces a much clearer and more robust ranking signal, which is better aligned with the needs of downstream heuristics and solvers.

## 4.3 Intra-Constraint Competitive GNN

Standard GNN message passing tends to smooth features across connected nodes, an effect that is counterproductive in the MILP context. As discussed in Section 3, variables sharing a constraint are not collaborators but competitors. An effective GNN architecture should therefore not homogenize its representations but instead *differentiate* them to highlight the most promising candidates for inclusion in a solution.

To achieve this, we propose that a variable's representation should be contextualized by its local competition. Instead of learning an absolute embedding, we aim to learn how each variable's features *deviate* from the average features of its direct competitors within each constraint. This relative representation is inherently more discriminative.

We implement this principle with our Intra-Constraint Competitive (ICC) layer. The ICC layer achieves differentiation through a simple yet effective normalization process that follows each standard GNN message-passing update. Let  $\boldsymbol{h}_j^{(l)}$  be the embedding of a variable  $v_j$  after the  $l^{\text{th}}$  message-passing layer. The ICC mechanism proceeds in three steps.

**Aggregate Competitor Features.** For each constraint  $c_k$ , we compute an aggregated message by averaging the embeddings of all variables participating in it:

$$\overline{\boldsymbol{h}}_{k}^{(l)} \leftarrow \frac{1}{|\mathcal{N}(c_{k})|} \sum_{v_{j} \in \mathcal{N}(c_{k})} \boldsymbol{h}_{j}^{(l)}, \tag{8}$$

where  $\mathcal{N}(c_k)$  denotes the set of variable nodes connected to constraint  $c_k$ . The vector  $\overline{\boldsymbol{h}}_k^{(l)}$  represents the "average competitor" within that constraint's neighborhood.

**Propagate Competitive Context.** The aggregated information is propagated back to the variables. Each variable  $v_j$  aggregates the "average competitor" representations from all constraints it participates in:

$$\overline{\boldsymbol{h}}_{j}^{(l)} \leftarrow \frac{1}{|\mathcal{N}(v_{j})|} \sum_{c_{k} \in \mathcal{N}(v_{j})} \overline{\boldsymbol{h}}_{k}^{(l)}, \tag{9}$$

where  $\mathcal{N}(v_j)$  is the set of constraint nodes connected to variable  $v_j$ . The resulting vector  $\overline{\boldsymbol{h}}_j$  represents the aggregated features of the average peer group against which variable  $v_j$  competes.

Compute Competitive Deviation The final update is then performed by subtracting the peer representation from the variable's embedding, scaled by a learnable parameter  $\beta$ :

$$\boldsymbol{h}_{i}^{(l)} \leftarrow \boldsymbol{h}_{i}^{(l)} - \beta \cdot \overline{\boldsymbol{h}}_{i}^{(l)} \tag{10}$$

This mechanism explicitly calculates the deviation of a variable's feature from its competitive baselines. A variable whose embedding is highly distinct from its peers will produce a resultant vector with a large magnitude, signaling it as a strong, standout candidate. Conversely, a variable that is feature-wise similar to its competitors will have its representation pushed towards the zero vector, diminishing its salience. This process directly counteracts the feature smoothing of standard GNNs and forces the model to learn embeddings that highlight the "winners" within each local competition, producing representations that are far more differentiated and informative for the final prediction task.

# 5 Experiments

In this section, we conduct extensive experiments to evaluate the effectiveness of CoCo-MILP. Our approach achieves significant improvements in solving performance on both the synthetic (Section 5.2) and real-world (Section 5.3) benchmarks, as well as generalization ability (Appendix E.4).

# 5.1 Experimental Setup

**Datasets** We evaluate our framework on four well-established MILP benchmarks frequently used in ML4CO research: Set Covering (SC), Item Placement (IP), Combinatorial Auctions (CA), and Workload Appointment (WA). These benchmarks cover a wide range of combinatorial structures, constraint types, and objective complexities. For SC and CA, we follow standard instance generation procedures from current works (Gasse et al. 2019; Wang et al. 2023; Han et al. 2023; Huang et al. 2024), while IP and WA are taken from the more challenging tracks of the NeurIPS 2021 ML4CO competition (Gasse et al. 2022a). Following the experimental setting in (Han et al. 2023), we use 240 instances for training, 60 for validation, and 100 for testing. Please refer to Appendix D.1 for further benchmark details.

Baselines We mainly evaluate our method through two standard categories. First, we measure the performance gains by integrating the heuristics learned by CoCo-MILP into two typical solvers, Gurobi (Gurobi Optimization 2021) and SCIP (Achterberg 2009). Second, we compare CoCo-MILP against two representative learning-based baselines: Predict-and-Search (PS) (Han et al. 2023) and Contrastive Predict-and-Search (ConPS) (Huang et al. 2024). Both PS and ConPS follow a two-stage paradigm which first predicts partial solutions and then finds better primal solutions based on the Gurobi or SCIP solvers. ConPS extends PS by incorporating contrastive learning to enhance predictive quality. Neural Diving (ND) (Nair et al. 2020a) is another related baseline with a similar structure to PS, but we do not include it in our comparison due to its weaker performance reported in PS. Most importantly, we are aware of recent stronger baselines, notably Apollo-MILP (Liu et al. 2025b), which focuses on improving search efficiency without modifying the training process of PS. Therefore, to demonstrate the compatibility of our method, we also integrate CoCo-MILP into Apollo-MILP as a plug-in component and report the results in Appendix E.5. More experimental details can be found in Appendix D.

**Metrics** To evaluate solution quality, we compare the best objective values (OBJ) obtained by each method within a

1000-second time limit on each test instance. To approximate the optimal value, we adopt the setting from Han et al. (2023), where a single-threaded Gurobi is executed for 3600 seconds and its best result is recorded as the best-known solution (BKS). We then compute the absolute primal gap as  $\text{gap}_{\text{abs}} := |\text{OBJ} - \text{BKS}|$ , which quantifies how far a solution is from the BKS. A smaller gapabs reflects higher solution quality under the same time budget.

Training and Inference Following the setup in PS, all methods are trained for 1000 epochs on each dataset, with the best model selected based on validation prediction loss. To enhance traditional solvers, PS introduces additional constraints to confine the solution space within a trust region, which is controlled by several key hyperparameters. However, since our benchmarks are more challenging and complex, the hyperparameter settings reported in the original papers result in poor performance. Therefore, we re-tune the hyperparameters for all baselines on our benchmarks. The final hyperparameters are detailed in Appendix D.3. And the extensive analysis of these parameters is presented in Appendix E.2.

#### 5.2 Main Evaluation

Solving Performance Table 1 presents comprehensive results demonstrating that our method consistently achieves state-of-the-art performance across all benchmarks. On the SC benchmark, our method exactly matches the BKS with a near-zero primal gap, yielding a 93.8% improvement over vanilla Gurobi. For the industrial-scale IP and WA benchmarks, our method achieves perfect optimality, fully matching BKS values. Even on the more complex CA benchmark, our approach narrows the absolute gap by 37.1% compared to Gurobi. In comparison with learning-based methods, our model reduces the primal gap by 78.6% against PS and 63.0% against ConPS, underscoring the effectiveness of our architecture in enhancing traditional solvers.

Primal Gap as a Function of Runtime As shown in Figure 6, our method demonstrates strong convergence across all benchmarks. Although the initial gap reduction appears less sharp, this is primarily due to the scaling of the x-axis. In practice, CoCo-MILP is able to reach high-quality solutions within the first 100 seconds. This behavior is attributed to the more accurate variable selection in our method. The fixed variables predicted by CoCo-MILP provide a better starting point for the solver, enabling more efficient local search. In contrast, baseline methods often make early decisions based on pointwise training losses, which can misidentify key variables and lead to premature convergence toward suboptimal solutions. The consistently better final objective values achieved by CoCo-MILP further support its advantage in both convergence speed and solution quality. In addition, we provide the results obtained with the SCIP solver for comparison, as presented in Appendix E.3.

#### 5.3 Evaluation on Real-world Benchmark

To further evaluate CoCo-MILP's applicability, we conduct experiments on the MIPLIB dataset (Gleixner et al. 2021). Following (Wang et al. 2023; Liu et al. 2025b), we focus on

Table 1: Performance comparison on four MILP benchmarks (CA, SC, IP, and WA) under a 1000-second time limit. '↑' indicates higher is better; '↓' indicates lower is better. **Bold** denotes the best result. All improvements are reported as gap<sub>abs</sub> relative to Gurobi.

	CA (BKS 97524.37)		SC (BK	KS 125.05) IP (BI		S 11.16)	WA (BKS 703.05)	
	Obj ↑	gap <sub>abs</sub> ↓	Obj↓	$gap_{abs} \downarrow$	Obj↓	gap <sub>abs</sub> ↓	Obj↓	gap <sub>abs</sub> ↓
Gurobi	97228.93	295.44	125.21	0.16	11.43	0.27	703.47	0.42
PS+Gurobi	97286.29	238.08	125.17	0.12	11.40	0.24	703.47	0.42
ConPS+Gurobi	97315.83	208.54	125.18	0.13	11.36	0.20	703.47	0.42
CoCo-MILP+Gurobi	97338.64	185.73	125.06	0.01	11.26	0.10	703.14	0.09
Improvement		37.1%		93.8%		63.0%		78.6%

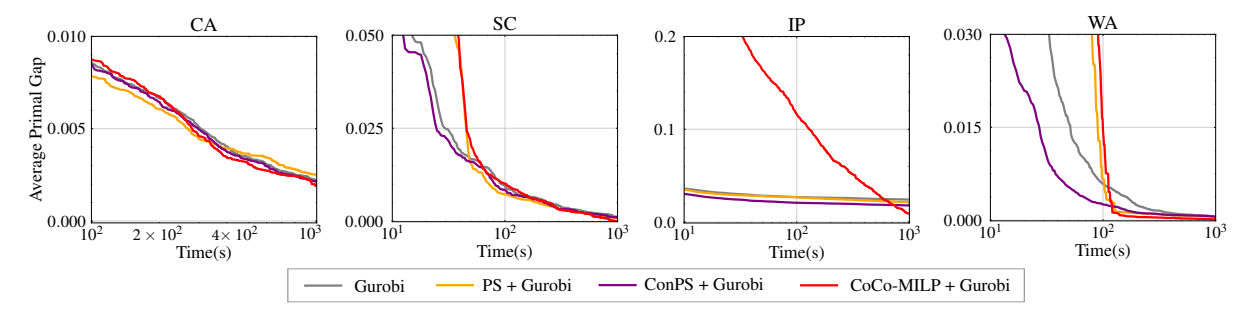


Figure 6: The average primal gap of each method over 100 test instances as a function of solving time. All methods are implemented using Gurobi, with a time limit of 1000 seconds.

the IIS subset of MIPLIB, which contains six training instances and five testing instances. The complete information about the MIPLIB benchmark, please refer to Appendix D.1. All methods are trained identically, and their performance is reported in Table 2. We also evaluate CoCo-MILP on additional challenging subsets of MIPLIB and report the results in Appendix E.1.

Table 2: The best objectives found by the approaches on each test instance in MIPLIB. We obtain the *BKS* from the website of MIPLIB. The ML approaches are implemented using Gurobi with a time limit set to 1000 seconds.

	BKS	Gurobi	PS	ConPS	CoCo-MILP
ex1010-pi	233.00	239.00	241.00	239.00	237.00
fast0507	174.00	174.00	179.00	179.00	174.00
ramos3	186.00	233.00	225.00	225.00	224.00
scpj4scip	128.00	132.00	133.00	133.00	131.00
scpl4	259.00	277.00	275.00	275.00	273.00

#### 5.4 Ablation Study

To evaluate the contribution of each component in CoCo-MILP, we compare the full model with four ablated variants: (i) Replacing the VCL loss with  $\mathcal{L}_{BCE}$ ; (ii) Removing the ranking terms; (iii) Removing the MCSL terms; (iv) Removing the ICC layers in the GNN. As shown in Table 3,

omitting either the VCL loss or ICC layers significantly degrades performance, confirming that these design elements play a critical role in CoCo-MILP's effectiveness.

Table 3: Ablation studies. The ML approaches are implemented using Gurobi with a time limit set to 1000 seconds. '↑' indicates that higher is better, and '↓' indicates that lower is better. We mark the **best values** in bold.

	SC (BKS 125.05)	CA (BKS 97524.37)
CoCo-MILP w.i. $\mathcal{L}_{BCE}$	125.25	97240.00
CoCo-MILP w/o $\mathcal{L}_{rank}$	125.21	97272.41
CoCo-MILP w/o $\mathcal{L}_{MSCL}$	125.19	97217.40
CoCo-MILP w/o $\mathcal{L}_{ICC\ layer}$	125.18	97315.96
CoCo-MILP	125.06	97338.64

# 6 Conclusion

In this paper, we summarize the limitations of current learning-based methods and propose CoCo-MILP to address through explicit modeling of inter-variable contrast and intra-constraint competition. Experiments demonstrate that CoCo-MILP outperforms other ML-based approaches, exhibiting promising real-world applicability.

# 7 Acknowledgments

This work was supported by the National Natural Science Foundation of China (NSFC, 72571284, 72421002, 62206303, 62273352), the Hunan Provincial Fund for Distinguished Young Scholars (2025JJ20073), the Science and Technology Innovation Program of Hunan Province (2023RC3009), the Foundation Fund Program of National University of Defense Technology (JS24-05), the Major Science and Technology Projects in Changsha, China (kq2301008), and the Hunan Provincial Innovation Foundation for Postgraduate (XJQY2025044).

# References

- Achterberg, T. 2009. SCIP: solving constraint integer programs. *Mathematical Programming Computation*, 1: 1–41.
- Bachman, P.; Hjelm, R. D.; and Buchwalter, W. 2019. Learning representations by maximizing mutual information across views. *Advances in neural information processing systems*, 32.
- Balas, E.; and Ho, A. 1980. Set covering algorithms using cutting planes, heuristics, and subgradient optimization: a computational study. Springer.
- Chechik, G.; Sharma, V.; Shalit, U.; and Bengio, S. 2010. Large scale online learning of image similarity through ranking. *Journal of Machine Learning Research*, 11(3).
- Chen, T.; Kornblith, S.; Norouzi, M.; and Hinton, G. 2020. A simple framework for contrastive learning of visual representations. In *International conference on machine learning*, 1597–1607. PmLR.
- Chen, Z.; Chen, X.; Liu, J.; Wang, X.; and Yin, W. 2024a. Expressive power of graph neural networks for (mixed-integer) quadratic programs. *arXiv* preprint *arXiv*:2406.05938.
- Chen, Z.; Liu, J.; Chen, X.; Wang, W.; and Yin, W. 2024b. Rethinking the capacity of graph neural networks for branching strategy. *Advances in Neural Information Processing Systems*, 37: 123991–124024.
- Chen, Z.; Liu, J.; Wang, X.; Lu, J.; and Yin, W. 2022. On representing linear programs by graph neural networks. *arXiv preprint arXiv:2209.12288*.
- Fan, C.; Shen, M.; Nussinov, Z.; Liu, Z.; Sun, Y.; and Liu, Y.-Y. 2023. Searching for spin glass ground states through deep reinforcement learning. *Nature communications*, 14(1): 725.
- Fan, C.; Zeng, L.; Sun, Y.; and Liu, Y.-Y. 2020. Finding key players in complex networks through deep reinforcement learning. *Nature machine intelligence*, 2(6): 317–324.
- Gasse, M.; Bowly, S.; Cappart, Q.; Charfreitag, J.; Charlin, L.; Chételat, D.; Chmiela, A.; Dumouchelle, J.; Gleixner, A.; Kazachkov, A. M.; Khalil, E.; Lichocki, P.; Lodi, A.; Lubin, M.; Maddison, C. J.; Christopher, M.; Papageorgiou, D. J.; Parjadis, A.; Pokutta, S.; Prouvost, A.; Scavuzzo, L.; Zarpellon, G.; Yang, L.; Lai, S.; Wang, A.; Luo, X.; Zhou, X.; Huang, H.; Shao, S.; Zhu, Y.; Zhang, D.; Quan, T.; Cao, Z.; Xu, Y.; Huang, Z.; Zhou, S.; Binbin, C.; Minggui, H.; Hao, H.; Zhiyu, Z.; Zhiwu, A.; and Kun, M. 2022a. The

- Machine Learning for Combinatorial Optimization Competition (ML4CO): Results and Insights. In Kiela, D.; Ciccone, M.; and Caputo, B., eds., *Proceedings of the NeurIPS 2021 Competitions and Demonstrations Track*, volume 176 of *Proceedings of Machine Learning Research*, 220–231. PMLR.
- Gasse, M.; Bowly, S.; Cappart, Q.; Charfreitag, J.; Charlin, L.; Chételat, D.; Chmiela, A.; Dumouchelle, J.; Gleixner, A.; Kazachkov, A. M.; et al. 2022b. The machine learning for combinatorial optimization competition (ml4co): Results and insights. In *NeurIPS 2021 competitions and demonstrations track*, 220–231. PMLR.
- Gasse, M.; Chételat, D.; Ferroni, N.; Charlin, L.; and Lodi, A. 2019. Exact combinatorial optimization with graph convolutional neural networks. *Advances in neural information processing systems*, 32.
- Geng, Z.; Li, X.; Wang, J.; Li, X.; Zhang, Y.; and Wu, F. 2023. A Deep Instance Generative Framework for MILP Solvers Under Limited Data Availability. In *Advances in Neural Information Processing Systems*.
- Geng, Z.; Wang, J.; Li, X.; Zhu, F.; HAO, J.; Li, B.; and Wu, F. 2025. Differentiable Integer Linear Programming. In *The Thirteenth International Conference on Learning Representations*.
- Gleixner, A.; Hendel, G.; Gamrath, G.; Achterberg, T.; Bastubbe, M.; Berthold, T.; Christophel, P.; Jarck, K.; Koch, T.; Linderoth, J.; et al. 2021. MIPLIB 2017: data-driven compilation of the 6th mixed-integer programming library. *Mathematical Programming Computation*, 13(3): 443–490.
- Gurobi Optimization, L. 2021. Gurobi optimizer. *URL http://www. gurobi. com.*
- Han, Q.; Yang, L.; Chen, Q.; Zhou, X.; Zhang, D.; Wang, A.; Sun, R.; and Luo, X. 2023. A gnn-guided predict-and-search framework for mixed-integer linear programming. In *The Eleventh International Conference on Learning Representations*.
- He, H.; Daume III, H.; and Eisner, J. M. 2014. Learning to search in branch and bound algorithms. *Advances in neural information processing systems*, 27.
- Hjelm, R. D.; Fedorov, A.; Lavoie-Marchildon, S.; Grewal, K.; Bachman, P.; Trischler, A.; and Bengio, Y. 2018. Learning deep representations by mutual information estimation and maximization. *arXiv preprint arXiv:1808.06670*.
- Huang, T.; Ferber, A.; Tian, Y.; Dilkina, B. N.; and Steiner, B. 2023. Searching Large Neighborhoods for Integer Linear Programs with Contrastive Learning. In *International Conference on Machine Learning*.
- Huang, T.; Ferber, A. M.; Zharmagambetov, A.; Tian, Y.; and Dilkina, B. 2024. Contrastive Predict-and-Search for Mixed Integer Linear Programs. In Salakhutdinov, R.; Kolter, Z.; Heller, K.; Weller, A.; Oliver, N.; Scarlett, J.; and Berkenkamp, F., eds., *Proceedings of the 41st International Conference on Machine Learning*, volume 235 of *Proceedings of Machine Learning Research*, 19757–19771. PMLR.
- Jiang, C.; Shu, X.; Qian, H.; Lu, X.; Zhou, J.; Zhou, A.; and Yu, Y. 2024. LLMOPT: Learning to Define and Solve Gen-

- eral Optimization Problems from Scratch. arXiv preprint arXiv:2410.13213.
- Khalil, E. B.; Morris, C.; and Lodi, A. 2022. Mip-gnn: A data-driven framework for guiding combinatorial solvers. In *Proceedings of the AAAI Conference on Artificial Intelligence*, volume 36, 10219–10227.
- Kuang, Y.; Wang, J.; Liu, H.; Zhu, F.; Li, X.; Zeng, J.; Jianye, H.; Li, B.; and Wu, F. 2024. Rethinking Branching on Exact Combinatorial Optimization Solver: The First Deep Symbolic Discovery Framework. In *The Twelfth International Conference on Learning Representations*.
- Labassi, A. G.; Chetelat, D.; and Lodi, A. 2022. Learning to Compare Nodes in Branch and Bound with Graph Neural Networks. In Koyejo, S.; Mohamed, S.; Agarwal, A.; Belgrave, D.; Cho, K.; and Oh, A., eds., *Advances in Neural Information Processing Systems*, volume 35, 32000–32010. Curran Associates, Inc.
- Land, A. H.; and Doig, A. G. 2010. An automatic method for solving discrete programming problems. Springer.
- Leyton-Brown, K.; Pearson, M.; and Shoham, Y. 2000. Towards a universal test suite for combinatorial auction algorithms. In *Proceedings of the 2nd ACM Conference on Electronic Commerce*, 66–76.
- Li, S.; Ouyang, W.; Paulus, M. B.; and Wu, C. 2023. Learning to Configure Separators in Branch-and-Cut. In *Thirty-seventh Conference on Neural Information Processing Systems*.
- Li, X.; Zhu, F.; Zhen, H.-L.; Luo, W.; Lu, M.; Huang, Y.; Fan, Z.; Zhou, Z.; Kuang, Y.; Wang, Z.; et al. 2024. Machine learning insides optverse ai solver: Design principles and applications. *arXiv preprint arXiv:2401.05960*.
- Liu, H.; Kuang, Y.; Wang, J.; Li, X.; Zhang, Y.; and Wu, F. 2023. Promoting Generalization for Exact Solvers via Adversarial Instance Augmentation. arXiv:2310.14161.
- Liu, H.; Wang, J.; Cai, Y.; Han, X.; Kuang, Y.; and HAO, J. 2025a. OptiTree: Hierarchical Thoughts Generation with Tree Search for LLM Optimization Modeling. In *The Thirty-ninth Annual Conference on Neural Information Processing Systems*.
- Liu, H.; Wang, J.; Geng, Z.; Li, X.; Zong, Y.; Zhu, F.; HAO, J.; and Wu, F. 2025b. Apollo-MILP: An Alternating Prediction-Correction Neural Solving Framework for Mixed-Integer Linear Programming. In *The Thirteenth International Conference on Learning Representations*.
- Liu, H.; Wang, J.; Zhang, W.; Geng, Z.; Kuang, Y.; Li, X.; Li, B.; Zhang, Y.; and Wu, F. 2024a. MILP-StuDio: MILP Instance Generation via Block Structure Decomposition. In *The Thirty-eighth Annual Conference on Neural Information Processing Systems*.
- Liu, S.; Fan, C.; Cheng, K.; Wang, Y.; Cui, P.; Sun, Y.; and Liu, Z. 2024b. Inductive meta-path learning for schemacomplex heterogeneous information networks. *IEEE Transactions on Pattern Analysis and Machine Intelligence*.
- Liu, S.; He, Y.; Wang, H.; Yang, W.; Wang, Y.; Cui, P.; and Liu, Z. 2025c. Environment Inference for Learning Generalizable Dynamical Systems. In *Advances in Neural Information Processing Systems*, volume 39.

- Mitchell, J. E. 2002. Branch-and-cut algorithms for combinatorial optimization problems. *Handbook of applied optimization*, 1(1): 65–77.
- Nair, V.; Bartunov, S.; Gimeno, F.; Von Glehn, I.; Lichocki, P.; Lobov, I.; O'Donoghue, B.; Sonnerat, N.; Tjandraatmadja, C.; Wang, P.; et al. 2020a. Solving mixed integer programs using neural networks. *arXiv preprint arXiv:2012.13349*.
- Nair, V.; Bartunov, S.; Gimeno, F.; Von Glehn, I.; Lichocki, P.; Lobov, I.; O'Donoghue, B.; Sonnerat, N.; Tjandraatmadja, C.; Wang, P.; et al. 2020b. Solving mixed integer programs using neural networks. *arXiv preprint arXiv:2012.13349*.
- Oord, A. v. d.; Li, Y.; and Vinyals, O. 2018. Representation learning with contrastive predictive coding. *arXiv preprint arXiv:1807.03748*.
- Pu, T.; Chen, C.; Zeng, L.; Liu, S.; Sun, R.; and Fan, C. 2024a. Solving Combinatorial Optimization Problem Over Graph Through QUBO Transformation and Deep Reinforcement Learning. In 2024 IEEE International Conference on Data Mining (ICDM), 390–399. IEEE.
- Pu, T.; Fan, C.; Shen, M.; Lu, Y.; Zeng, L.; Nussinov, Z.; Chen, C.; and Liu, Z. 2024b. Exploratory Combinatorial Optimization Problem Solving via Gauge Transformation. In 2024 IEEE International Conference on Data Mining (ICDM), 821–826. IEEE.
- Pu, T.; Geng, Z.; Liu, H.; Liu, S.; Wang, J.; Zeng, L.; Chen, C.; and Fan, C. 2025. RoME: Domain-Robust Mixture-of-Experts for MILP Solution Prediction across Domains. In *The Thirty-ninth Annual Conference on Neural Information Processing Systems*.
- Qu, Q.; Li, X.; Zhou, Y.; Zeng, J.; Yuan, M.; Wang, J.; Lv, J.; Liu, K.; and Mao, K. 2022. An improved reinforcement learning algorithm for learning to branch. *arXiv preprint arXiv*:2201.06213.
- Schroff, F.; Kalenichenko, D.; and Philbin, J. 2015. Facenet: A unified embedding for face recognition and clustering. In *Proceedings of the IEEE conference on computer vision and pattern recognition*, 815–823.
- Song, J.; lanka, r.; Yue, Y.; and Dilkina, B. 2020. A General Large Neighborhood Search Framework for Solving Integer Linear Programs. In Larochelle, H.; Ranzato, M.; Hadsell, R.; Balcan, M.; and Lin, H., eds., *Advances in Neural Information Processing Systems*, volume 33, 20012–20023. Curran Associates, Inc.
- Sonnerat, N.; Wang, P.; Ktena, I.; Bartunov, S.; and Nair, V. 2021. Learning a Large Neighborhood Search Algorithm for Mixed Integer Programs. *ArXiv*, abs/2107.10201.
- Wang, H.; Liu, H.; Luo, J.; Wang, J.; et al. 2024. Accelerating PDE Data Generation via Differential Operator Action in Solution Space. In *Forty-first International Conference on Machine Learning*.
- Wang, H.; Wang, J.; Ma, M.; Shao, H.; and Liu, H. 2025. SymMaP: Improving Computational Efficiency in Linear Solvers through Symbolic Preconditioning. In *The Thirty-ninth Annual Conference on Neural Information Processing Systems*.

- Wang, Z.; Li, X.; Wang, J.; Kuang, Y.; Yuan, M.; Zeng, J.; Zhang, Y.; and Wu, F. 2023. Learning Cut Selection for Mixed-Integer Linear Programming via Hierarchical Sequence Model. In *The Eleventh International Conference on Learning Representations*.
- Wu, Y.; Song, W.; Cao, Z.; and Zhang, J. 2021. Learning Large Neighborhood Search Policy for Integer Programming. In Ranzato, M.; Beygelzimer, A.; Dauphin, Y.; Liang, P.; and Vaughan, J. W., eds., *Advances in Neural Information Processing Systems*, volume 34, 30075–30087. Curran Associates, Inc.
- Ye, H.; Xu, H.; and Wang, H. 2024. Light-MILPopt: Solving Large-scale Mixed Integer Linear Programs with Lightweight Optimizer and Small-scale Training Dataset. In *The Twelfth International Conference on Learning Representations*.
- Ye, H.; Xu, H.; Wang, H.; Wang, C.; and Jiang, Y. 2023. GNN&GBDT-Guided Fast Optimizing Framework for Large-scale Integer Programming. In Krause, A.; Brunskill, E.; Cho, K.; Engelhardt, B.; Sabato, S.; and Scarlett, J., eds., *Proceedings of the 40th International Conference on Machine Learning*, volume 202 of *Proceedings of Machine Learning Research*, 39864–39878. PMLR.
- Ye, M.; Wang, J.; Zhu, F.; Wang, Z.; Kuang, Y.; Li, X.; Luo, W.; Hao, J.; and Wu, F. 2025. Dynamic Configuration for Cutting Plane Separators via Reinforcement Learning on Incremental Graph. In *The Thirty-ninth Annual Conference on Neural Information Processing Systems*.
- Zhang, B.; Fan, C.; Liu, S.; Huang, K.; Zhao, X.; Huang, J.; and Liu, Z. 2024. The Expressive Power of Graph Neural Networks: A Survey. *IEEE Transactions on Knowledge & Data Engineering*, (01): 1–20.
- Zhang, S.; Zeng, S.; Li, S.; Wu, F.; and Li, X. 2025. Learning to Select Nodes in Branch and Bound with Sufficient Tree Representation. In *The Thirteenth International Conference on Learning Representations*.

# **Appendix**

# **A** Extensive Analysis of Motivations

**Inter-Variable Logits Ambiguity** In many practical combinatorial optimization problems, the items or objects we are interested in are inherently sparse. This means the set of variables assigned a value of 1 is significantly smaller than the set of variables assigned a value of 0. The binary cross-entropy training objective treats the prediction for each variable as an independent binary classification problem. By focusing on each variable in isolation, the model is not explicitly incentivized to create a large separation between the scores (logits) of positive-class variables and negative-class ones. As a result, many variables from the negative set can receive higher scores than variables from the positive set, leading to a significant overlap in their logit distributions and a failure to establish a clear global decision boundary.

**Neglect of Intra-Constraint Competitions** We analyze the cause of the issue. The design of standard GNN message-passing mechanisms inherently causes feature smoothing, a process where the representations of connected nodes become more similar after each layer of aggregation. In the bipartite graph representation of a MILP, variables that appear in the same constraint are immediate (1-hop) neighbors of that constraint node. Consequently, the GNN's smoothing effect is direct and strong, tending to homogenize the representations of these variables.

**Explanation under the OR Context** The need to differentiate variables within a constraint is common in combinatorial optimization.

- First, this principle of competition is common in diverse real-world problems, such as scheduling, planning, logistics, and network design. For example, in scheduling, a single machine can only perform one job at a time, making the jobs competitors for that time slot. In logistics and network design, choosing to build a warehouse in one location or select one delivery route competitively excludes other options.
- Second, many canonical MILP formulations are built upon constraints that enforce strict differentiation. For example, one of the most common structures in combinatorial optimization, the set-packing constraint, is explicitly defined as  $\sum_{x_i \in S} x_i \leq 1$ . The assignment constraints ensure that each worker can only be assigned one task, i.e.,  $\sum_j x_{ij} = 1$ . The knapsack or budget constraints only select a small subset of items in the candidates, i.e.,  $\sum_i w_i x_i \leq W$ . While the specific formulations differ, the underlying principle of competition among variables governed by a single logical or resource-based constraint is a cornerstone of MILP modeling.

The inability of standard GNNs to capture these essential competitive dynamics motivates the development of a specialized architecture, the Intra-Constraint Competitive (ICC) GNN layer, which is explicitly designed to differentiate these competing variable representations.

## **B** Related Works

Machine Learning for MILPs Machine learning has been widely applied to accelerate the solving process of MILPs. Existing methods can be roughly classified into two categories: machine learning inside an exact solver and machine learning for solution prediction. In the first category, researchers apply machine learning models to replace certain heuristics for acceleration. These works include learning to branch (Gasse et al. 2019; Khalil, Morris, and Lodi 2022; Kuang et al. 2024), learning for cut selection and separation (Wang et al. 2023; Li et al. 2023), learning to select nodes (Labassi, Chetelat, and Lodi 2022; He, Daume III, and Eisner 2014), and so on. These works have demonstrated significant improvement under an exact solver framework. The second category of the works focuses on directly predicting a solution for MILP. These methods first use a neural network to predict a high-quality partial solution, and then search in a neighborhood of the partial solution (Nair et al. 2020a; Han et al. 2023; Huang et al. 2024). The neighborhood search process greatly reduces the search space and thus has gained more and more popularity.

Contrastive Learning Contrastive learning has emerged as a powerful technique to learn embeddings that pull similar (positive) samples together and push dissimilar (negative) samples apart. Contrastive learning achieves the goal by designing the contrastive functions. For pair-wise contrastive learning, triplet loss (Chechik et al. 2010; Schroff, Kalenichenko, and Philbin 2015) was designed to learn embeddings by ensuring that an anchor sample is closer to a positive sample than to a negative sample by a certain margin. The multiple-pair contrastive loss extended this by using multiple negative samples for each positive pair, leading to more efficient training. The InfoNCE loss (Bachman, Hjelm, and Buchwalter 2019; Hjelm et al. 2018; Oord, Li, and Vinyals 2018), a key component in many modern contrastive methods, is derived from noise-contrastive estimation and aims to maximize the mutual information between different views of the data. The NT-Xent loss (Chen et al. 2020), a normalized temperature-scaled cross-entropy loss, is a popular variant that has been widely adopted. In our work, contrastive learning directly addresses the challenge of ambiguous predictions by directly maximizing the relative difference between variables that should be 1 and 0.

# C Implementation Details

## **C.1** Graph Representation

Following prior work (Gasse et al. 2019; Han et al. 2023), we represent each MILP instance as a weighted bipartite graph  $\mathcal{G} = (\mathcal{V} \cup \mathcal{W}, \mathcal{E})$ , where  $\mathcal{V}$  and  $\mathcal{W}$  denote the sets of variable nodes and constraint nodes, respectively, and  $\mathcal{E}$  represents the nonzero entries in the constraint matrix. Each node and edge in the bipartite graph is associated with a set of numerical features derived from MILP coefficients and structural statistics. Our design closely follows the feature definitions used in previous works, and we adopt the same preprocessing pipeline without modification. These features provide rich information for the GNN to exploit the structure of MILP instances effectively.

#### **C.2** Model Architecture

Our model builds upon the GNN encoder architecture proposed by Bachman, Hjelm, and Buchwalter (2019), which is also adopted in recent works (Han et al. 2023; Geng et al. 2025; Liu et al. 2025b). Given a bipartite graph  $\mathcal{G} = (\mathcal{V} \cup \mathcal{W}, \mathcal{E})$ , we initialize the node and edge embeddings as:

$$h_{v_i}^{(0)} = \text{MLP}_{\theta}(v_i), \quad h_{w_i}^{(0)} = \text{MLP}_{\theta}(w_j), \quad h_{e_{ij}} = \text{MLP}_{\theta}(e_{ij}).$$
 (11)

Then we apply K layers of half-convolutions:

$$h_{w_i}^{(k+1)} \leftarrow \text{MLP}_{\theta} \left( h_{w_i}^{(k)}, \sum_{j: e_{ij} \in \mathcal{E}} \text{MLP}_{\phi} \left( h_{w_i}^{(k)}, h_{e_{ij}}, h_{v_j}^{(k)} \right) \right),$$
 (12)

$$h_{v_j}^{(k+1)} \leftarrow \text{MLP}_{\phi} \left( h_{v_j}^{(k)}, \sum_{i: e_{ij} \in \mathcal{E}} \text{MLP}_{\phi} \left( h_{w_i}^{(k+1)}, h_{e_{ij}}, h_{v_j}^{(k)} \right) \right).$$
 (13)

After each message passing layer, we insert our Intra-Constraint Competitive (ICC) module to model exclusion among variables within the same constraint. Specifically, for each variable  $v_i$ , we compute:

$$\bar{h}_j^{(k)} = \frac{1}{|\mathcal{N}(v_j)|} \sum_{c \in \mathcal{N}(v_j)} \left( \frac{1}{|\mathcal{N}(c)|} \sum_{v \in \mathcal{N}(c)} h_v^{(k)} \right),\tag{14}$$

$$h_{v_j}^{(k)} \leftarrow h_{v_j}^{(k)} - \beta \cdot \bar{h}_j^{(k)},$$
 (15)

where  $\beta$  is a learnable scalar.

After K layers, we apply a concatenation-based Jumping Knowledge (JK) mechanism to obtain the final representations:

$$h_{v_i} = \text{MLP}_{\theta} \left( \text{CONCAT}_{k=0}^K h_{v_i}^{(k)} \right), \tag{16}$$

$$z_{v_i} = \text{MLP}_{\theta}(h_{v_i}), \tag{17}$$

where  $z_{v_i}$  is the predicted logit for variable  $v_i$ , followed by a sigmoid to obtain the marginal probability.

The ICC module introduces minimal additional overhead, as it only requires one scalar parameter  $\beta$  per layer and reuses intermediate embeddings from the base architecture.

# C.3 Implementation of our method and the baselines

We compare CoCo-MILP against two recent state-of-the-art learning-based approaches: Predict-and-Search (PS)(Han et al. 2023) and its contrastive variant ConPS(Huang et al. 2024). For PS, we directly adopt the official implementation provided by the authors, including the encoder architecture. As ConPS does not release its source code, we reproduce its framework based on the algorithmic details in the original paper. To ensure fair comparison, we carefully re-tuned its hyperparameters and verified the reproduced performance against reported results. In our implementation of ConPS, the positive-to-negative sample ratio is set to 1:10, and negative samples are drawn from low-quality feasible solutions. All experiments are conducted under a consistent computational environment, using an NVIDIA GeForce RTX 3090 GPU and Intel(R) Xeon(R) Gold 5320 CPU (26 cores, 2.20GHz).

# D Experimental Details

#### **D.1** Details of Benchmarks

**Main Evaluation.** The CA and SC benchmark instances are constructed based on standard procedures used in prior works. In particular, the CA instances follow the generation algorithm from (Leyton-Brown, Pearson, and Shoham 2000), and the SC instances are derived using the approach proposed in (Balas and Ho 1980), as summarized in (Gasse et al. 2019). For the IP and WA benchmarks, we adopt the instance set released as part of the NeurIPS 2021 ML4CO competition (Gasse et al. 2022b). Table 4 summarizes the key statistics of all benchmark instances used in our paper.

	# Constraint	# Variable	# Binary Variables	# Continuous Variables	# Integer Variables
CA	2593	1500	1500	0	0
SC	3000	5000	5000	0	0
IP	195	1083	1050	33	0
WA	64306	61000	1000	60000	0

Table 4: Statistical information of the benchmarks we used in this paper.

Generalization. To evaluate the cross-scale generalization capacity of our method, we construct a new set of large-scale instances for the CA and SC benchmarks. These instances are synthesized using publicly available generation tools from prior work (Gasse et al. 2019). The constructed CA problems contain approximately 2,600 constraints and 4,000 variables on average, while the SC problems are built with around 6,000 constraints and 10,000 variables. Compared to the training set, these evaluation instances are significantly larger in both dimensionality and combinatorial complexity, providing a more rigorous test for evaluating model transferability across instance scales.

MIPLIB Subset. To evaluate the effectiveness of CoCo-MILP on real-world combinatorial problems, we construct a benchmark based on selected instances from the MIPLIB 2017 dataset (Gleixner et al. 2021). MIPLIB contains a diverse collection of challenging MILP problems drawn from practical domains such as transportation, energy, logistics, and industrial design. Due to the dataset's structural heterogeneity, directly training on the full set is often infeasible for learning-based methods. We adopt an instance similarity-based selection strategy, consistent with prior work such as Apollo-MILP (Liu et al. 2025b). Specifically, similarity is computed using 100 hand-crafted instance features, as introduced in Gleixner et al. (2021). Following this protocol, we first utilize the IIS subset from MIPLIB, which consists of eleven real-world instances. Among them, six are used for training—glass-sc, iis-glass-cov, 5375, 214, 56133, and iis-hc-cov—and five are used for testing, namely ex1010-pi, fast0507, ramos3, scpj4scip, and scpl4. To further challenge the model's generalization ability, we extend our evaluation to a new set of larger and more difficult MIPLIB instances. For each selected test instance, we construct a training set by identifying approximately five similar instances based on the same feature similarity criteria. All models are trained on these instance-specific training sets and then evaluated on their corresponding target instances. Table 5 summarizes the detailed statistics of the full set of test instances used in our MIPLIB benchmark. The instances span a wide range in terms of size, including both medium- and large-scale problems. Notably, the variable types vary across instances, covering binary, general integer, and continuous variables. This diversity enables us to assess the robustness and versatility of CoCo-MILP across different variable domains. Experimental results (see Appendix D) confirm that CoCo-MILP consistently accelerates solution quality, regardless of variable type.

#### **D.2** Training Details

Like previous work (Han et al. 2023), our approach maintain the same parameters with (Han et al. 2023) without introducing too many extra parameters. We mainly introduce three parameters in CoCo-MILP to control the ranking loss weight, minority variable re-weighting coefficient, and inter-class margin size respectively whose analysis are reported in Appendix E.2. The key parameters in training are summarized in Table 6.

#### **D.3** Inference Details

To ensure a fair comparison and strong empirical performance, we report the inference-time hyperparameters used by all methods across benchmarks in Table 7. Each method uses a tuple  $(k_0, k_1, \Delta)$ , where  $k_0$  and  $k_1$  determine the top-ranked variable candidates for fixing and unfixing, and  $\Delta$  controls the  $\ell_1$ -norm trust region for solution refinement. For CoCo-MILP, we perform moderate tuning of these hyperparameters on the validation set of each benchmark to account for the increased complexity and scale of our datasets compared to prior works. While existing baselines such as PS and ConPS provide default hyperparameters in their original papers, we find that these settings often underperform on our harder synthetic and real-world benchmarks. Therefore, we re-tune the parameters for PS and ConPS to ensure their best possible performance under our experimental setup. This tuning procedure significantly improves their feasibility rate and solution quality, and the final configurations are reported in Table 7. We also refer readers to our sensitivity analysis in Appendix E.2, where we study the impact of  $(k_0, k_1, \Delta)$  on final performance. These results indicate that CoCo-MILP is relatively robust to moderate hyperparameter changes and

Table 5: Statistical information of the instances in the constructed MIPLIB dataset.

	# Constraint	# Variable	# Binaries	# Integers	# Continuous	# Nonzero Coefficient
ex1010-pi	1468	25200	25200	0	0	102114
fast0507	507	63009	63009	0	0	409349
ramos3	2187	2187	2187	0	0	32805
scpj4scip	1000	99947	99947	0	0	999893
scpl4	2000	200000	200000	0	0	2000000
dws008-03	16344	32280	18928	0	13352	165168
dws008-01	6064	11096	6608	0	4488	56400
bab2	17245	147912	147912	0	0	2027726
bab5	4964	21600	21600	0	0	155520
bab6	29904	114240	114240	0	0	1283181
neos-3555904-turama	146493	37461	37461	0	0	793605
neos-3656078-kumeu	17656	14870	9755	4455	660	59292
supportcase17	2108	1381	732	235	414	5253
fastxgemm-n2r7s4t1	6972	904	56	0	848	22584
tr12-30	750	1080	360	0	720	2508

Table 6: Hyperparameters used in our experiments.

Name	Value	Description
embed_size	64	The embedding size of the GNN encoder.
num_epochs	1000	Number of max running epochs.
lr	0.0001	Learning rate for training.
$\lambda_{ m rank}$	0.01	Regularization coefficient, namely the coefficient for Rank Loss.
au	0.1	The temperature hyperparameter in MSCL.
$\gamma$	0.9	The margin hyperparameter in Rank loss for CA,SC and WA, as for IP, we set $\gamma$ to 0.6

achieves competitive results across a wide range of values. All inference experiments are conducted using Gurobi 11.0.3 with a single thread (i.e., Threads=1) and setting the solver focus to solution quality (MIPFocus=1). For experiments involving SCIP, we similarly use single-threaded execution to maintain consistency.

Table 7: Hyperparameters of  $(k_0, k_1, \Delta)$  used in this paper.

Benchmark	CA	SC	IP	WA
PS+Gurobi	(600,0,1)	(2000,0,100)	(400,5,10)	(0,500,10)
ConPS+Gurobi	(900,0,50)	(1000,0,200)	(400,5,3)	(0,500,10)
CoCo-MILP+Gurobi	(400, 0, 40)	(1000, 0, 200)	(60, 35, 55)	(20, 200, 100)
PS+SCIP	(400,0,10)	(2000,0,100)	(400,5,1)	(0,600,5)
ConPS+SCIP	(900,0,50)	(1000,0,200)	(400,5,3)	(0,400,50)
CoCo-MILP+SCIP	(400, 0, 40)	(1000, 0, 200)	(60, 35, 55)	(20, 200, 100)

# **E** Additional results

#### E.1 Real-world Datasets

To further verify the real-world applicability of CoCo-MILP, we evaluate its performance on a selected subset of MIPLIB. Due to the high heterogeneity of this dataset, we follow prior work (Liu et al. 2025b) and select a group of structurally similar instances that resemble our synthetic benchmarks. For each test instance, we construct a training set by identifying approximately five nearby instances based on structural similarity, such as the number of variables, constraints, and sparsity patterns. This instance-wise adaptation enables the model to generalize effectively without the need for global retraining. During inference, we adopt fixed hyperparameters across all runs:  $k_0 = 0.7$ ,  $k_1 = 0.1$ , and  $\Delta = 800$ . These settings are consistent with our main evaluation and are not tuned per instance, highlighting the robustness of CoCo-MILP. As shown in Table 8, CoCo-MILP matches or improves upon all baselines on nearly every instance. Notably, it achieves the BKS in all five MIPLIB test cases where the baseline methods fall short. These results confirm that CoCo-MILP maintains strong performance even in challenging real-world scenarios.

Table 8: The best objectives found by the approaches on each test instance in MIPLIB. *BKS* represents the best objectives from the website of MIPLIB.

	BKS	Gurobi	PS+Gurobi	ConPS+Gurobi	CoCo-MILP+Gurobi
dws008-03	62831.76	64452.67	71234.06	67473.85	66047.78
dws008-01	37412.60	37412.60	39043.26	38817.50	38486.10
bab2	-357544.31	-357538.58	-357449.20	-357544.31	-357544.31
bab5	-106411.84	-106411.84	-106411.84	-106411.84	-106411.84
bab6	-284248.23	-284248.23	-284224.56	-284224.56	-284248.23
neos-3555904-turama	-34.7	-34.7	-34.7	-34.7	-34.7
neos-3656078-kumeu	-13172.2	-13171.3	-13114.0	-13120.6	-13172.20
supportcase17	1330.00	1330.00	1330.00	1330.00	1330.00
fastxgemm-n2r7s4t1	42.00	42.00	42.00	42.00	42.00
tr12-30	130596.00	130596.00	130596.00	130596.00	130596.00

## **E.2** Hyperparameter Analysis

To gain a deeper understanding of CoCo-MILP, we conduct a comprehensive analysis of key hyperparameters, including the regularization coefficient  $\lambda_{\text{Rank}}$ , the ranking margin  $\gamma$ , the temperature parameter  $\alpha$ , and the inference-related hyperparameters  $k_0$ ,  $k_1$ , and  $\Delta$ .

Regularization Coefficient  $\lambda_{\text{Rank}}$  This coefficient controls the weight of the pairwise ranking loss in the overall contrastive objective. We vary  $\lambda_{\text{Rank}}$  in the range [0.01, 0.08] and evaluate its effect on the CA benchmark. As shown in Table 10, increasing the emphasis on inter-class separation does not always improve solution quality. A large coefficient may increase the influence of outliers, such as variables that are correctly classified but located far from their class centers. This can lead to greater inter-class distances while simultaneously reducing overall accuracy. These results suggest that focusing solely on inter-class separation is not sufficient; it is equally important to ensure that samples within the same class are compactly clustered.

Table 9: Analysis of different regularization coefficients. The ML approaches are implemented using Gurobi, with a time limit set to 1000 seconds. '↑' indicates that higher is better, and '↓' indicates that lower is better. We mark the **best values** in bold.

	CA (BKS	CA (BKS 97524.37)					
	Obj↑ gap <sub>abs</sub> .						
0.01	97338.64	185.73					
0.03	97245.94	278.43					
0.05	97171.55	352.82					
0.08	97237.85	250.52					

Margin  $\gamma$  in Ranking Loss The margin parameter  $\gamma$  determines the minimum separation enforced between positive and negative variable logits. We observe in Table 10 that increasing  $\gamma$  from 0.6 to 0.9 steadily improves performance. A larger margin better avoids ambiguous predictions around 0.5, thereby enhancing decision reliability and yielding more accurate final solutions.

Table 10: Analysis of different margins. The ML approaches are implemented using Gurobi, with a time limit set to 1000 seconds. '↑' indicates that higher is better, and '↓' indicates that lower is better. We mark the **best values** in bold.

	CA (BKS	CA (BKS 97524.37)					
	Obj↑ gap <sub>abs</sub>						
0.6	97264.81	259.56					
0.7	97237.65	250.72					
0.8	97295.39	228.72					
0.9	97338.64	185.73					

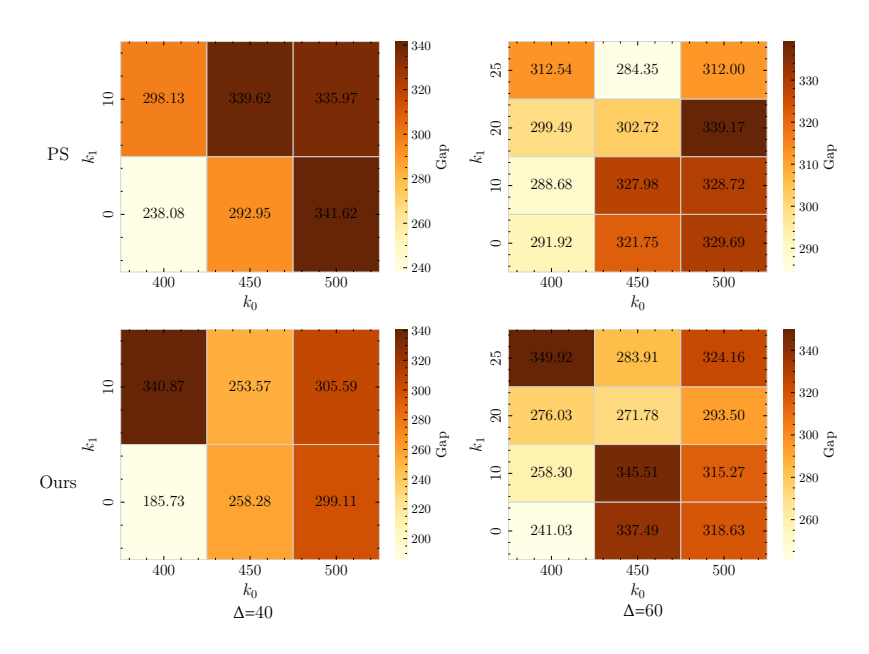


Figure 7: Impact of inference hyperparameters  $k_0$ ,  $k_1$ , and  $\Delta$  on CA benchmark. Each cell reports the average absolute primal gap to BKS under a 1000-second time limit. Upper panels correspond to the PS baseline; lower panels correspond to CoCoMILP. Smaller values indicate better performance.

**Temperature**  $\alpha$  **in Multi-Sample Contrastive Loss** The temperature parameter  $\alpha$  adjusts the sharpness of the softmax function in the contrastive loss. Smaller values focus the loss more on hard examples. As shown in Table 11, the best performance is achieved at  $\alpha = 0.1$ , while both overly low (e.g., 0.05) and high values (e.g., 0.5) degrade solution quality. This confirms that careful tuning of temperature is important to balance hard-negative emphasis and training stability.

Table 11: Analysis of different temperatures. The ML approaches are implemented using Gurobi, with a time limit set to 1000 seconds. '↑' indicates that higher is better, and '↓' indicates that lower is better. We mark the **best values** in bold.

	CA (BKS	CA (BKS 97524.37)					
	Obj↓	gap <sub>abs</sub> ↓					
0.05	97216.59	0.12					
0.1	97338.64	185.73					
0.2	97127.90	396.47					
0.3	97258.12	266.25					
0.5	97281.20	243.17					

Inference Hyperparameters  $k_0$ ,  $k_1$ , and  $\Delta$  We further analyze the impact of inference hyperparameters, namely the top- $k_0$  and top- $k_1$  candidate sets for variable selection, and the trust region radius  $\Delta$ . These parameters jointly determine the search space for the solver after the prediction stage. We evaluate their influence on the CA benchmark by measuring the absolute gap to the BKS under different configurations. The results are visualized as heatmaps in Figure 7, where smaller values indicate better solution quality. Compared to the PS baseline, CoCo-MILP consistently achieves smaller gaps across all settings. Notably, when  $\Delta=40$ , our method obtains the best performance at  $(k_0=400,k_1=0)$  with a gap of 185.73. This suggests that the predictions produced by CoCo-MILP are already of high quality and require less reliance on extensive neighborhood search. On the other hand, when  $\Delta$  increases to 60, the benefit of larger trust regions diminishes for CoCo-MILP, while the baseline shows more sensitivity to this change. Overall, these findings confirm that CoCo-MILP not only improves prediction quality but also stabilizes inference performance under varying search parameters.

#### **E.3** Evaluation on More Solvers

To further validate the robustness and generality of CoCo-MILP, we evaluate its performance under the SCIP solver, using the same benchmark setup and a 1000 seconds time limit. The results are summarized in Table 12. Compared to the vanilla SCIP

solver, CoCo-MILP+SCIP consistently improves the primal solution quality across all benchmarks. Specifically, on the SC benchmark, our method reduces the primal gap from 1.48 to 1.21, and on CA, the absolute gap drops by 41.19. For the more challenging IP and WA benchmarks, CoCo-MILP+SCIP achieves notable gap reductions of 0.41 and 0.64, respectively. These results further demonstrate the compatibility of CoCo-MILP with different solvers and its effectiveness as a plug-in predictor, capable of improving solution quality even when integrated into alternative solver backends beyond Gurobi.

Table 12: Performance comparison on four popular MILP benchmarks using SCIP solver, under a 1000 seconds time limit. ' $\uparrow$ ' indicates higher is better; ' $\downarrow$ ' indicates lower is better. **Bold** denotes the best result. All improvements are reported as gap<sub>abs</sub> relative to *BKS*.

	CA (BKS 97524.37)		SC (BKS 125.05)		IP (BKS 11.16)		WA (BKS 703.05)	
	Obj ↑	gap <sub>abs</sub> ↓	Obj↓	gap <sub>abs</sub> ↓	Obj↓	gap <sub>abs</sub> ↓	Obj ↓	$gap_{abs} \downarrow$
SCIP	96423	1100.47	126.43	1.48	16.55	5.39	705.77	2.72
PS+SCIP	96426.46	1097.91	126.65	1.60	16.18	5.02	705.21	2.16
ConPS+SCIP	96428.83	1095.54	126.40	1.35	16.16	5.00	705.21	2.16
CoCo-MILP+SCIP	96465.09	1059.28	126.26	1.21	16.14	4.98	705.13	2.08

#### E.4 Generalization

To further evaluate the generalization ability of CoCo-MILP, we test its performance on larger CA and SC instances, which contain significantly more constraints and variables, as described in Appendix D.1. We directly apply the model trained on the main evaluation set to these larger instances without any fine-tuning. The results are reported in Table 13, demonstrating that CoCo-MILP exhibits strong generalization capability to larger and more complex problem instances.

Table 13: Generalization results of 100 larger instances on CA and SC using Gurobi with a 1000 seconds time limit. '↑' indicates that higher is better, and '↓' indicates that lower is better. We mark the **best values** in bold.

	CA (BKS 115787.97)		SC (BKS 101.45)	
	Obj ↑	gap <sub>abs</sub> ↓	Obj↓	gap <sub>abs</sub> ↓
Gurobi	114960.25	827.72	102.29	0.84
PS+Gurobi	115228.20	559.77	102.27	0.82
ConPS+Gurobi	115343.23	444.74	102.18	0.73
CoCo-MILP+Gurobi	115463.49	324.48	101.91	0.46

# **E.5** Plug-in with other techniques

To demonstrate the flexibility and broad applicability of CoCo-MILP, it is worth highlighting that our method can be easily integrated with other techniques to achieve enhanced performance. Below, we present two approaches.

**Intra-constraint Competition in the Search Phase** As analyzed in Section 3, modeling intra-constraint competition can significantly improve model performance. A straightforward extension is to apply logit normalization during the search phase, mimicking the effect of ICC layers to amplify the differences among variables within the same constraint. We conduct additional experiments on the SC benchmark, and the results are reported in Table 15. These results demonstrate that incorporating intra-constraint competition into the search phase can lead to further performance improvements.

Table 14: Results of intra-constraint competition in search phase. The ML approaches are implemented using Gurobi, with a time limit set to 1000 seconds. '↑' indicates that higher is better, and '↓' indicates that lower is better. We mark the **best values** in bold.

	SC (BKS 125.05)	
	Obj ↓	gap <sub>abs</sub> ↓
PS+Gurobi	125.17	0.12
CoCo-MILP+Gurobi	125.06	0.01
CoCo-MILP+Search Competition+Gurobi	125.05	0.00

Plug-in with the Stronger Baseline As a promising direction in the ML4CO field, we observe that increasingly powerful methods have been proposed, such as Apollo-MILP (Liu et al. 2025b) and DiffILO (Geng et al. 2025). Among them, Apollo-MILP is a representative framework that achieves strong performance under the predict-and-search paradigm. It adopts a prediction-and-correction strategy to improve solution quality during the search phase, without altering the training process. The original Apollo-MILP is built upon PS (Han et al. 2023). To evaluate the compatibility of CoCo-MILP, we integrate it into Apollo-MILP by replacing the PS predictor with CoCo-MILP, while keeping the inference hyperparameters unchanged. We conduct experiments on the SC benchmark, and the results are reported in Table 15. When CoCo-MILP is used as a plug-in to enhance Apollo-MILP, the resulting system achieves solutions that match the BKS exactly. This demonstrates the strong complementarity between our method and advanced search frameworks, and further confirms the effectiveness and generality of CoCo-MILP.

Table 15: Results of CoCo-MILP enhancing with Apollo-MILP. The ML approaches are implemented using Gurobi, with a time limit set to 1000 seconds. '↑' indicates that higher is better, and '↓' indicates that lower is better. We mark the **best values** in bold.

	SC (BK	SC (BKS 125.05)		
	Obj↓	gap <sub>abs</sub> ↓		
PS+Gurobi	125.17	0.12		
CoCo-MILP+Gurobi	125.06	0.01		
Apollo-MILP+Gurobi	125.08	0.03		
CoCo-MILP+Apollo-MILP+Gurobi	125.05	0.00		